Supplementary Information

Dorsolateral prefrontal cortex and amygdala function during cognitive reappraisal predicts weight restoration and emotion regulation impairment in anorexia nervosa

Trevor Steward*[1,2,3], Ignacio Martínez-Zalacaín*[3,4], Gemma Mestre-Bach[2,3,8], Isabel Sánchez[2,3], Nadine Riesco[2,3], Susana Jiménez-Murcia[2,3,4], Jose A Fernández-Formoso[2], Misericordia Veciana de las Heras[5], Nuria Custal[3], Jose M Menchón[3,4,7], Carles Soriano-Mas[#3,6,7], Fernando Fernandez-Aranda[#2,3,4]

[1]Melbourne School of Psychological Sciences, Faculty of Medicine, Dentistry and Health Sciences, University of Melbourne, Australia
[2]Ciber Fisiopatología Obesidad y Nutrición (CIBEROBN), Instituto Salud Carlos III, Barcelona, Spain
[3] Department of Psychiatry, Bellvitge University Hospital -IDIBELL, Barcelona, Spain
[4]Department of Clinical Sciences, School of Medicine, University of Barcelona, Barcelona, Spain
[5]Neurology Department, Bellvitge University Hospital-IDIBELL, Barcelona, Spain
[6]Department of Psychobiology and Methodology. Universitat Autònoma de Barcelona, Barcelona, Spain
[7]Ciber Mental Health (CIBERSAM), Instituto Salud Carlos III, Barcelona, Spain
[8]Universidad Internacional de La Rioja, La Rioja, Spain

[*]These authors contributed equally to this work.

[#]Corresponding authors:
Dr. Fernando Fernández-Aranda, PhD & Dr. Carles Soriano-Mas, PhD
Department of Psychiatry, Bellvitge University Hospital/IDIBELL, Barcelona, Spain;
Email: ffernandez@bellvitgehospital.cat & csoriano@idibell.cat
Phone: +34-93-2607227

Supplementary Information

fMRI Acquisition and Preprocessing

MRI scans were conducted using a 3T Phillips Ingenia system equipped with a thirty-two-channel phased-array head coil. The functional MRI (fMRI) sequence used single-shot gradient-echo echo-planar imaging (EPI), with a repetition time of 2000 msec, an echo time of 25 msec, and a pulse angle of 90°, in a 24-cm field of view and an 80 × 80-pixel matrix, providing isotropic voxel sizes of 3 × 3 × 3 mm, with no gap. 40 interleaved sections, parallel to the anterior-posterior commissure line, were acquired for each whole-brain volume. A high-resolution T1-weighted anatomical scan was also acquired to facilitate registration of EPI data into standard MNI space and for extracting individual global grey matter volume. Specifically, we used a three-dimensional fast-spoiled gradient, inversion-recovery sequence with 233 contiguous slices (repetition time, 10.43 msec; echo time, 4.8 msec; flip angle, 8°) in a 24-cm field of view, with a 320 × 320 pixel matrix and isotropic voxel sizes of 0.75 × 0.75 x 0.75 mm.

All functional images were initially preprocessed using the Wavelet Despike procedure within the BrainWavelet Toolbox to remove high and low frequency artifacts induced by abrupt physical movements (Patel *et al.* 2014). Remaining image processing was performed using Statistical Parametric Mapping software (SPM12, Wellcome Department of Imaging Neuroscience, London, England; www.fil.ion.ucl.ac.uk/spm) toolbox running on MATLAB R2017a. Functional images underwent slice timing correction and were then realigned to the mean position of all scans and co-registered to their respective T1 images, which were used for normalization to MNI space. Next, normalization parameters were applied to the functional time-series, which were finally smoothed with an 8-mm full width at half maximum (FWHM) kernel. Movement parameters, white matter, cerebrospinal fluid (CSF), and global blood oxygen level-dependent (BOLD) time-series were introduced as confounders in a further denoising step performed using the CONN toolbox (Whitfield-Gabrieli & Nieto-Castanon 2012).

Grey matter volume

Global grey matter volumes were extracted using the *Segment* function included in SPM12 (Ashburner & Friston 2005). Individual gray matter segments in native space were then analyzed with an in-house script for calculating the number of voxels in (and, therefore, the total volume of) each grey matter segment. This value was used as a nuisance covariate in the analyses. Two-sample T-tests comparing HC and AN patients were performed, showing that participants in the AN group had significantly lower global grey matter volumes than HC ($t=2.88$, $p=0.006$).

Emotion regulation task

Prior to scanning, participants were given instruction on how to utilize reappraisal strategies. Three types of reinterpretations were recommended using an example situation: (1) the scene is not real (e.g. the people on the screen are actors); (2) the situation will

likely get better with time; and (3) the situation is not as grave as it first appears (e.g. seeing the situation in a more positive light). Participant were specifically instructed that they were not to use non-cognitive strategies (i.e. as looking away) during stimulus presentation.

During scanning, each block began with the instructive prompt (LookNeutral, LookNegative or Regulate) presented in the middle of the screen for four seconds. After the prompt, participants viewed two different pictures of equal valence for ten seconds each. After the presentation of the second picture of each block, the intensity of the participants' distress was self-rated on a 1–5 numeric scale (1 being 'neutral' and 5 being 'extremely negative') in order to confirm whether participants were successfully carrying out the task instructions.

24 images from the International Affective Picture System were used for the task (Lang *et al.* 2005): eight neutral pictures (e.g. household objects), which were presented in the LookNeutral condition, and 16 highly unpleasant pictures (e.g. mutilations) in the LookNegative and Regulate conditions. In total, the task consisted of twelve, 20-second blocks including the presentation of two images for ten seconds, with a total of four blocks for each condition. Instructions (LookNeutral, LookNegative or Regulate) were pseudo-randomized throughout the task to avoid the induction of sustained mood states. In-scanner ratings were recorded through an fMRI-compatible response pad (Lumina–Cedrus Corporation). Each block was followed by a 10-second presentation of a cross fixation to separate each block and to minimize carry-over effects. Task instructions and visual stimuli were presented using Presentation® software (Version 18.3, build 03.11.16, www. neurobs.com) through an MRI-compatible BOLD screen (BOLD screen 32, Cambridge Research Systems) located at the rear of the scanner gantry. An angled mirror system was used to allow participants to see the images.

Images were selected according to International Affective Picture System normative values for valence and arousal; mean valence values were 5.79 (0.71), 2.53 (0.69), 2.66 (0.68) and mean arousal values were 4.28 (0.73), 6.44 (0.46) and 6.40 (0.60) for images included in the LookNeutral, LookNegative, and Regulate conditions, respectively (Lang *et al.* 2005).

Psychopathology Scale

The Symptom Checklist 90-Revised (SCL-90-R; Derogatis 2002) was administered to evaluate a broad range of psychopathology symptoms. This test measures nine primary symptom dimensions, including depression and anxiety. Scores for the AN group can be found in Table S1.

Skin Conductance Response (SCR) Acquisition and Analysis

Using an EDA100c MRI module connected to a Biopac MP150 Amplifier (Biopac Systems Inc.), SCR signal was recorded from the volar surfaces of the distal phalanges of the third and fourth fingers of the participants' non-dominant hand, using two Ag-AgCl, non-polarizable electrodes attached to Velcro straps, and filled with Biopac isotonic (GEL101). Acquisition parameters were set to a gain of 5 μSiemens/Volt, the low pass filter to 10Hz,

the high pass filter to DC, and an acquisition sample rate of 250 Hz. Signal pre-processing was performed using AcqKnowledge 4.4.0 Software (Biopac Systems, Inc.) following a standard pipeline that consisted of down sampling to 65.2 Hz, smoothing by applying a median filter of 65 samples to eliminate movement artifacts and low pass filtering of 1Hz. A peak scoring analysis was performed for the SCR and was measured blind to the researcher regarding the condition being evaluated. A value was extracted and considered valid if there was an increase greater than 0.02s μSiemens and if it lasted at least 0.5 seconds within the scoring time window. For the images, the temporal window analyzed was defined between 1-20 s. of the onset of the first image of each condition block.

Table S1. Clinical Information: Anorexia Nervosa Group

	Anorexia nervosa group n=21	
Amenorrhea	Present: 11 (52.4%)	Absent: 10 (47.6%)
Tobacco Use	Yes: 9 (42.9%)	No: 12 (57.1)
Anorexia Nervosa Subtype	Restrictive:17 (80.9%)	Binge-eating/purging: 4 (19.1%)
Disorder Duration (years)	Mean: 3.93	SD: 3.17
Psychotropic Medication	Active: 6***** (28.6%)	None: 15 (71.4%)
Time from Admission to Scanning (days)	Mean: 14.91	SD: 7.51
SCL-90-R GSI	Mean: 1.74	SD: .67
SCL-90-R: Depression	Mean: 2.44	SD: .93
SCL-90-R: Anxiety	Mean: 1.81	SD: .79

*2 SSRIs; 2 SSRIs and benzodiazepines; 1 benzodiazepines; 1 SSRI & NaSSAs. SCL-90-R GSI: Symptom Checklist 90-Revised – Global Severity Index.

Table S2. Main Effects of LookNeg>LookNeutral in All Participants.

Ke[a]	peak t	MNI Coordinates			AAL Atlas Label
		x	y	z	
5448	13.42	46	-70	-2	Occipital_Inf_R
7699	9.85	-50	-72	0	Occipital_Mid_L
2270	7.72	20	-4	-14	Amygdala_R
314	5.30	0	60	26	Frontal_Sup_Medial_L
262	4.83	-20	-88	26	Occipital_Sup_L
142	4.62	44	28	-4	Frontal_Inf_Orb_R
153	4.60	44	10	24	Frontal_Inf_Oper_R
69	4.26	40	20	-36	Temporal_Pole_Mid_R
32	4.12	-18	-28	22	Caudate_L
76	4.05	8	12	56	Supp_Motor_Area_R
35	4.02	0	54	-24	Frontal_Sup_Orb_L
63	3.99	18	-24	14	Thalamus_R
13	3.86	-30	20	-16	Insula_L
23	3.83	-22	-48	-48	Cerebelum_9_L
20	3.68	22	-88	26	Occipital_Sup_R

Regions showing significant effects during the LookNeg>LookNeutral contrast of the emotion regulation task ($p < 0.001$, cluster extent >10); MNI: Montreal Neurological Institute. AAL: Automated anatomical labelling (Rolls *et al.* 2020); [a]Cluster extent in voxels.

Table S3. Main Effects of Regulate>LookNegative in All Participants.

Ke[a]	peak t	MNI Coordinates			AAL Atlas Region
		x	y	z	
307	5.38	-16	48	-12	Frontal_Sup_Orb_L
602	5.37	22	22	44	Frontal_Sup_R
272	5.23	-28	4	60	Frontal_Mid_L
562	5.12	56	-50	36	Angular_R
39	5.04	50	-8	-40	Temporal_Inf_R
199	4.80	66	-28	-6	Temporal_Mid_R
246	4.69	10	44	-14	Frontal_Med_Orb_R
34	4.55	-2	-2	-26	ParaHippocampal_L
34	4.54	-28	-68	54	Parietal_Sup_L
186	4.50	-44	-42	44	Parietal_Inf_L
102	4.31	36	36	34	Frontal_Mid_R
151	4.24	-58	-32	-6	Temporal_Mid_L
38	4.19	58	12	22	Frontal_Inf_Oper_R
69	3.94	2	-42	44	Precuneus_R

Regions showing significant effects during the LookNeg>LookNeutral contrast of the emotion regulation task ($p < 0.001$, cluster extent >10); MNI: Montreal Neurological Institute. AAL: Automated anatomical labelling (Rolls *et al.* 2020); [a]Cluster extent in voxels.

Supplementary Figure 1. Galvanic Skin Conductance Response Analysis

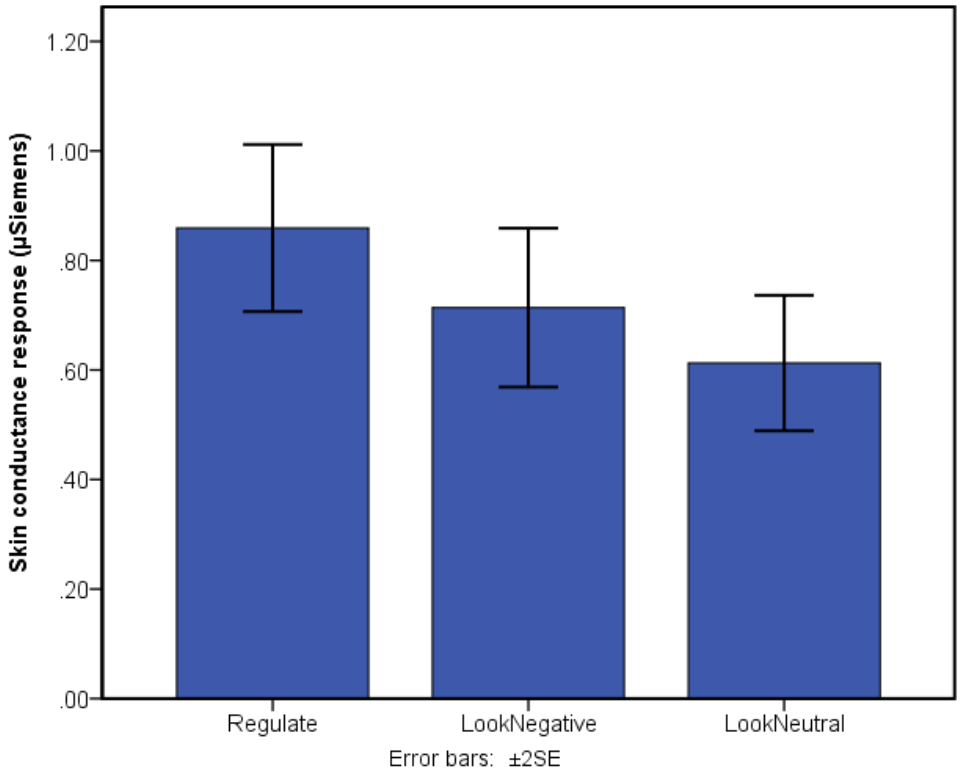

Bar plot (Mean±2SE) depicting skin conductance response (SCR) across the three task blocks. SCR during LookNegative blocks fell into a middle position, as evidenced by a significant linear increase across the three conditions (t=3.58, p=.002). SCR during Regulate blocks was significantly higher than during LookNeutral blocks (t=2.72, p=.002). No effect of group was found (F=3.25, p=.084).

Supplementary Figure 2:

Regulate>LookNegative Activation Patterns with and without Covarying for Global Grey Matter Volume (HC>AN)

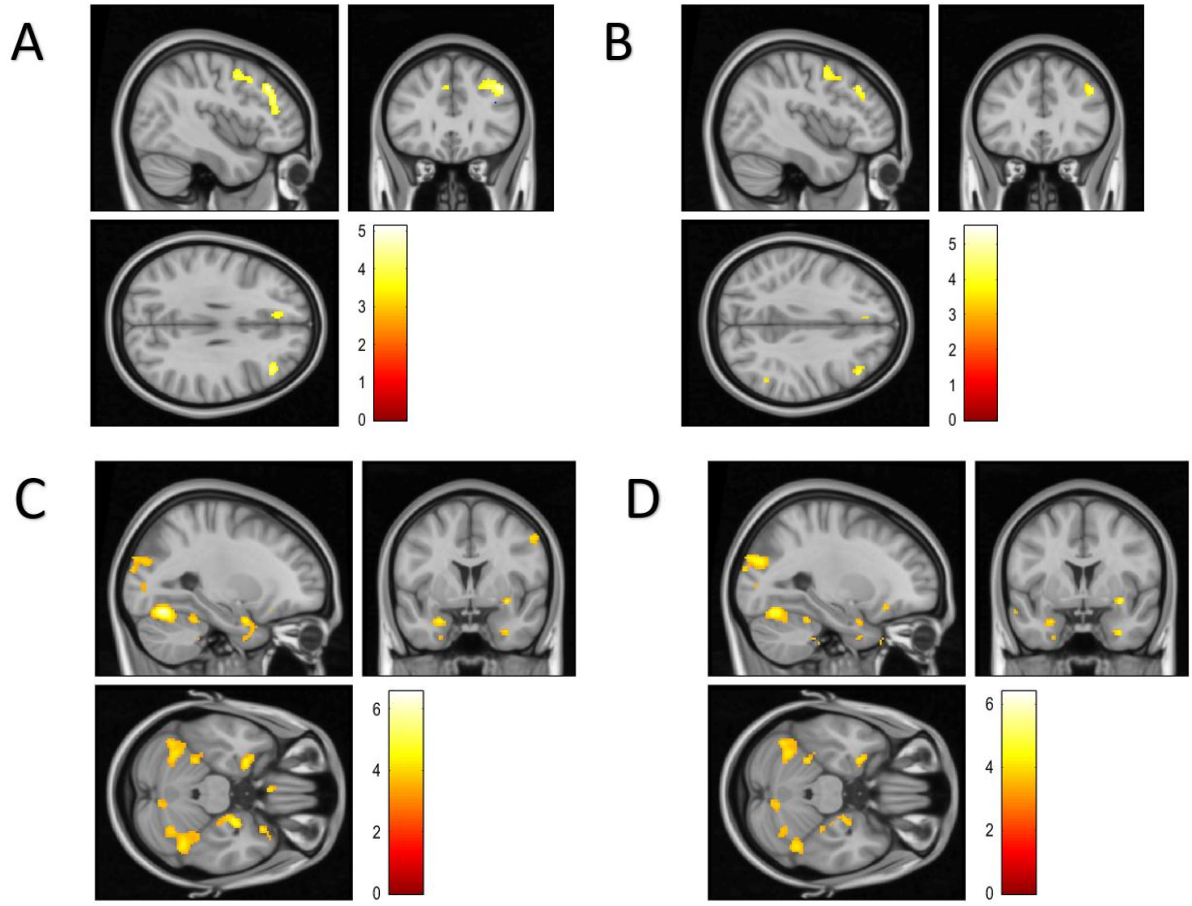

Comparison of activation patterns during Regulate>LookNegative when covarying (A) and not covarying (B) for global grey matter volume (HC>AN; $p<0.001$ uncorrected), and in dlPFC PPI connectivity during Regulate>LookNegative when covarying (C) and not covarying (D) for global grey matter volume (HC>AN; $p<0.001$ uncorrected).

Supplementary Figure 3:

Regulate>LookNegative Activation Patterns with and without Covarying for Psychotropic Medication Use (HC>AN)

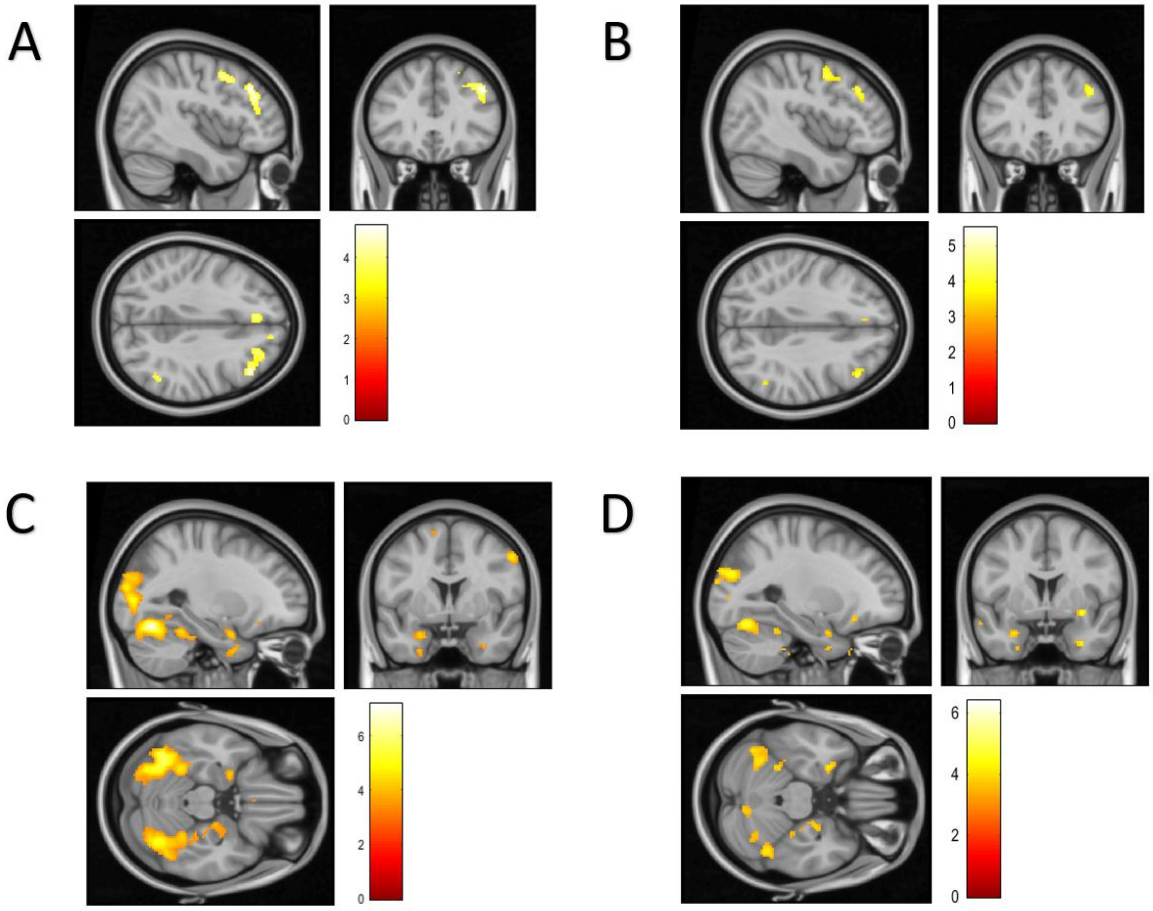

Comparison of activation patterns during Regulate>LookNegative when covarying (A) and not covarying (B) for psychotropic medication use (HC>AN; $p<0.001$ uncorrected), and in dlPFC PPI connectivity during Regulate>LookNegative when covarying (C) and not covarying (D) for psychotropic medication use (HC>AN; $p<0.001$ uncorrected).

Supplementary Figure 4. In-scanner distress ratings.

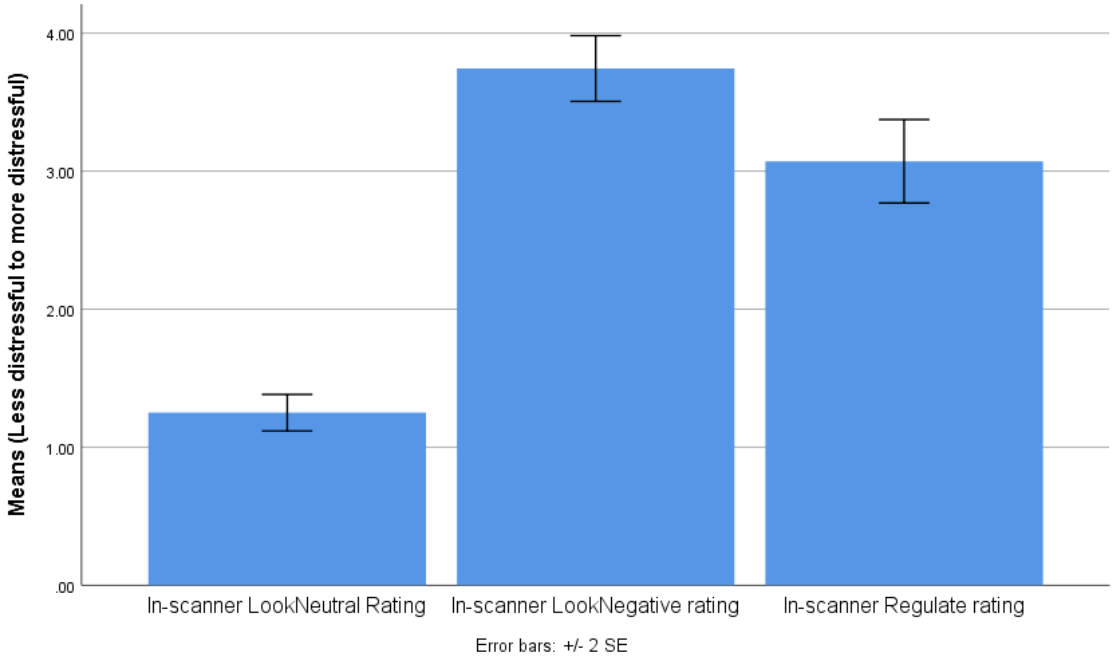

Bar plot (Mean±2SE) depicting in-scanner distress ratings across the three task conditions. Analysis of distress ratings for each condition (LookNeutral, LookNegative and Regulate) revealed a main effect of condition ($F_{(2, 39)}$ = 198.36, p<0.001). Post-hoc comparisons showed that LookNegative differed from LookNeutral, indicating negative emotion induction during this condition for both groups (LookNegative>LookNeutral: t= 20.9, p<0.001). Post-hoc comparisons between Regulate and LookNegative identified differences between the two conditions (LookNegative>Regulate t=4.78, p<0.001), indicating participants endorsed lower distress levels during blocks when instructed to use cognitive reappraisal. No significant effects of group ($F_{(1, 40)}$ = 2.55, p=0.118) were found.

Supplementary Figure 5:

Main Effects of Condition in All Participants from the Cognitive Reappraisal Task.

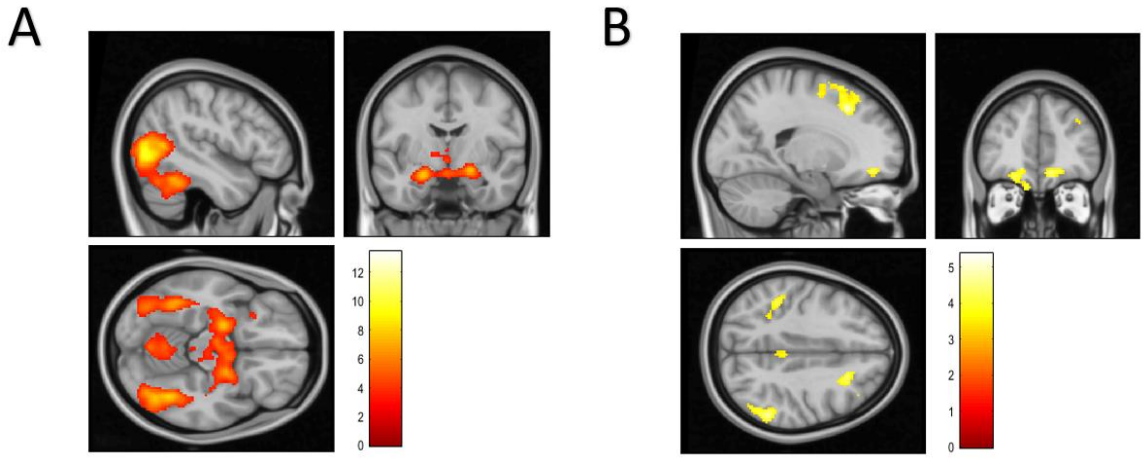

Main effect of condition (A) LookNegative>LookNeutral and (B) Regulate>LookNegative in all participants. ($p<0.001$ uncorrected; cluster extent>10)

References

Ashburner J, Friston KJ (2005). Unified segmentation. *NeuroImage* **26**, 839–851.
Derogatis L (2002). *SCL-90-R. Cuestionario de 90 síntomas-Manual*. TEA Editor. Madrid.
Lang P, Bradley M, Cuthbert B (2005). International Affective Picture System (IAPS): Digitized Photographs, Instruction Manual and Affective Ratings. Technical Report A-6. *2005*
Patel AX, Kundu P, Rubinov M, Jones PS, Vértes PE, Ersche KD, Suckling J, Bullmore ET (2014). A wavelet method for modeling and despiking motion artifacts from resting-state fMRI time series. *NeuroImage* **95**, 287–304.
Rolls ET, Huang CC, Lin CP, Feng J, Joliot M (2020). Automated anatomical labelling atlas 3. *NeuroImage*
Whitfield-Gabrieli S, Nieto-Castanon A (2012). *Conn* : A Functional Connectivity Toolbox for Correlated and Anticorrelated Brain Networks. *Brain Connectivity*